Summary of the 4th GISMO pool

I. Hermelo, C. Kramer, N. Billot, S. Leclercq and M. González

February 24, 2014

Abstract

The 4th Goddard-IRAM Superconducting 2 mm Observer camera (GISMO) pool took place from October 22nd to November 5th, 2013. During the first week of the pool the bad weather conditions heavily hindered the pool, allowing observations only for a total of 25.7 hours. During the second week the weather conditions were favorable, allowing to observe a total of 85.9 hours. Data for 10 of 11 projects were collected.

The median value of the opacities measured during the observations was $\tau_{225\,\mathrm{GHz}} = 0.307 \pm 0.226$. The 38% of the 1574 scans collected were taken for projects of the good weather queue (e.g., deep fields, star forming regions with faint extended structures, low-mass prestellar cores), 39% for projects of the bad weather queue (e.g., lensed galaxies, active galactic nucleus, supernova remnants), and the remaining 23% were taken under the "test" project, which was used when unstable weather conditions or technical problems did not allow to observe properly.

GISMO behavior during the 4th pool was good in terms of stability with the exception of a firmware issue on the GISMO server in the receiver cabin. This problem, which produces corrupted data, affected the observations several days without being noticed. Steve Maher has developed a new pipeline merging code that detects and corrects the corrupted data. All the scans taken during the 4th GISMO pool were reprocessed using the new pipeline and most of the corrupted data were recovered. To avoid this problem in future runs, a daily rebooting of the firmware will be included in the helium recycling routine.

The median value of healthy pixels was 101 and the median value of the noise equivalent flux density (NEFD) derived from the Nexus logsheet[1] was $16.8\,\mathrm{mJy}\,\sqrt{\mathrm{s}}$. The value of the NEFD measured for scans collected under good weather conditions is higher than the value measured under bad weather conditions. A total of 8 healthy scans on Uranus were considered to study the flux stability. The median value of the integrated flux density was 16.9 Jy, with an rms of 0.8 Jy (4.7%). From this value we derived a temperature brightness of $102.5 \pm 4.9\,\mathrm{K}$, in good agreement with the expected value of 106.6 K reported by Sayers et al. (2012).

After the run, Attila Kóvacs released a new version of `CRUSH` (v 2.15-2) including a new Jy/counts factor based on Uranus data, many fixes and workarounds for avoiding invalid data, correction of the positional information in each scan for the recorded tracking errors of the telescope, an updated pointing model based on the 4th GISMO pool data, as well as some other minor changes.

[1] I.e., data were reduced using crush v 2.15-1 and the `default` filtering option.

1 Pool statistics

A total of 302.5 hours were scheduled at the IRAM 30m radiotelescope for the 4th GISMO pool from Ocober 22nd to November 5th, 2013. Only 37% of the total amount of hours allocated were observed. Table 1 summarizes the statistics at the end of the pool.

We want to note that the analysis of the observed time described above it is based on the GISMO Nexus logsheet and therefore, it only includes the integration time on targets and pointing sources. In order to estimate the slewing time used to move the antenna between targets and pointing sources, $t_{\rm slew}$, we search in the GISMO Nexus logsheet for pointing scans preceded and followed by target scans. If $t_{\rm n}^{\rm point}$ is the time spent on the nth pointing scan, and $t_{\rm n-1}^{\rm fin}$ and $t_{\rm n+1}^{\rm ini}$ are the final and the initial time of the previous and the following target scans, respectively, then $t_{\rm slew}$ can be estimated as:

$$t_{\rm slew} = t_{\rm n-1}^{\rm fin} - t_{\rm n+1}^{\rm ini} - t_{\rm n}^{\rm point} \tag{1}$$

We found 48 occurrences of the sequence **target** $\rightarrow$ **pointing** $\rightarrow$ **target**. The median value of $t_{\rm slew}$ was 6.0 minutes. If we take into account $t_{\rm slew}$, the percentage of total time observed increases to 44% of the allocated time. Columns 7 and 8 of Table 1 show the observed time per project when we take into account the slewing time, which was estimated as $t_{\rm slew}$ times the number of pointing scans done plus the dead time between scans, $\rm t_{dead}$, times the total number of scans collected. Column 9 shows the total integration time on the target and column 10 is the percentage that this time represents in terms of the total time spent on the project. Depending on the observing strategy, the overheads (column 10) range from ~25% to ~40%.

Project			$t_{allocated}$	$t_{\rm observed}$		$t_{\rm real}$		$t_{\rm target}$	
ID	Priority	PI	h	h	%	h	%	h	%
(1)	(2)	(3)	(4)	(5)	(6)	(7)	(8)	(9)	(10)
077-13	5	CK	18.0	10.3	57.1	14.2	79.0	8.88	62.4
100-13	5	HD	50.0	17.6	35.2	22.7	45.4	15.95	70.3
103-13	5	JS	35.0	21.9	62.5	26.7	76.3	20.70	77.5
079-13	5	MAl	21.0	13.2	63.0	16.5	78.7	11.99	72.6
097-13	4	EA	18.0	1.6	8.6	1.9	10.5	1.49	78.6
096-13	4	FB	10.0	0.1	0.0	0.0	0.0	0.00	0.0
101-13	4	PF	30.0	4.3	14.5	5.5	18.5	3.97	71.5
099-13	3	AKo	40.0	16.3	40.7	21.3	53.3	14.68	68.9
078-13	3	IH	21.0	1.5	7.2	1.9	8.9	1.45	77.8
098-13	3	MAr	34.5	7.8	22.7	9.5	27.6	7.26	76.2
102-13	2	ED	25.0	17.0	68.2	20.7	82.7	15.61	75.5

Table 1: Statistics of the projects scheduled during the 4th GISMO pool. The three first columns correspond to the project name, the rate assigned by the IRAM program committee, and the initials of the PI, respectively. Column 4 is the total amount of allocated hours for each project. Columns 5 and 6 are the total amount of hours that the project was observed and its percentage of completion, respectively. Columns 7 and 8 give the same information than columns 5 and 6 but taking into account the slewing time and the dead time between scans. Finally, columns 9 and 10 correspond to the time spent on the target and the percentage that this time represents in terms of $t_{\rm real}$.

2 Pointing, focus and calibration

Pointing corrections were systematically done every 60-90 minutes during the 4th GISMO pool. The pointing scans consisted on $1.5' \times 1.5'$ Lissajous maps. The median value and the rms for the pointing corrections in azimuth and elevation are $\Delta\mathrm{Az} = 0.6 \pm 7.2$ and $\Delta\mathrm{El} = 0.0 \pm 4.7$, respectively. The pointing corrections for GISMO are larger than the typical values obtained with the heterodyne receivers. This is because the pointing model was not updated for GISMO. Nevertheless, pointing sources were always detected within the array, and in most of the cases the peak is located within the central pixel (see Figure 1).

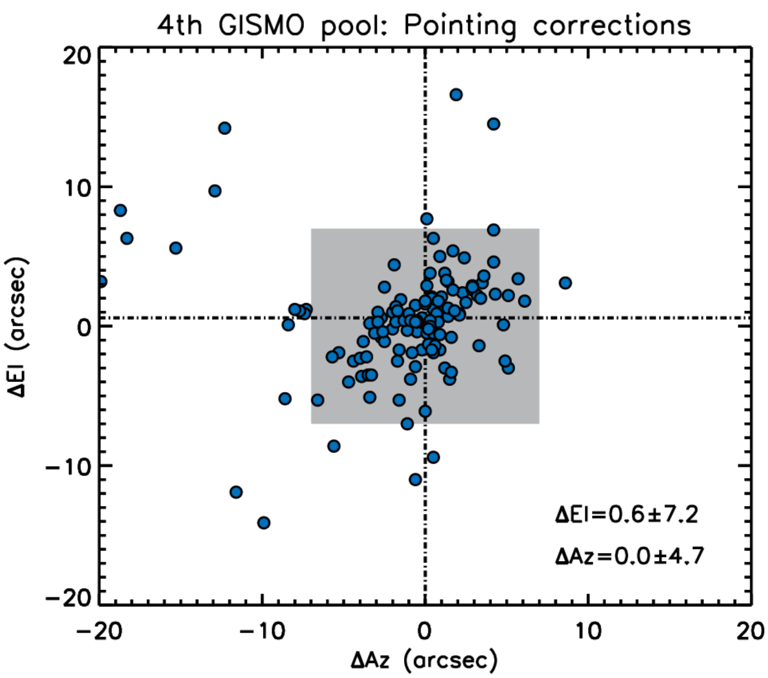

Figure 1: Pointing corrections applied during the GISMO pool. The gray shaded area represents the GISMO pixel size. The black dashed lines correspond to the median values found for ΔAz and ΔEl.

Focus corrections were based on five consecutive $1.5' \times 1.5'$ Lissajous maps taken at five different focus values ($\Delta\mathrm{Z}_{\mathrm{current}}$, $\Delta\mathrm{Z}_{\mathrm{current}} \pm 0.6\,\mathrm{mm}$, $\Delta\mathrm{Z}_{\mathrm{current}} \pm 1.2\,\mathrm{mm}$). Focus corrections were calculated with second order fits to the integrated intensity and the FWHM. The new value of the focus was determined as the value that maximizes the flux and minimizes the FWHM (see Hermelo et al. 2013 for details). The day time evolution of focus corrections were well behaved and predictable. The median value and the rms of the values used is $\Delta\mathrm{Z} = -1.8 \pm 0.8\,\mathrm{mm}$ (see Figure 2)

For the 4th GISMO pool Uranus was used as primary calibrator. A total of 8 healthy scans were collected (see Figure 3). It is important to mention that based on Uranus' observations from November 2nd and the Bendo et al. 2013 model, the Jy/counts factor was modified from the old value of 30.5 obtained during the 1st GISMO pool (see Bruni et al. 2012 for details) to the slightly lower value of 29.3. The median flux density of these scans, using the new Jy/counts factor, is 16.9 Jy and the rms is 0.8 Jy (4.7%). From this value it is possible to derive a brightness temperature of 102.5 K, which is 3.8% lower than the value of 106.6 K reported by Sayers et al. (2012) using Bolocam data collected between 2003 and 2010.

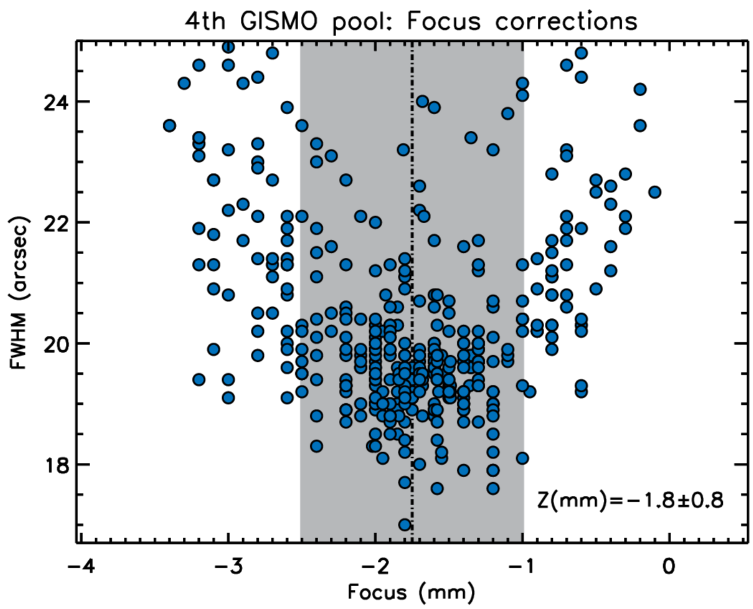

Figure 2: Focus corrections used during the GISMO pool. The vertical black dashed line and the gray shaded area correspond to the median value and to the rms, respectively.

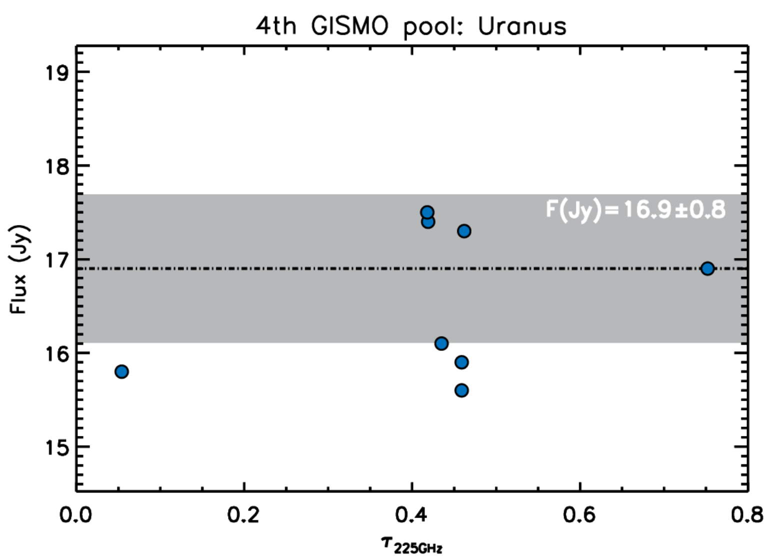

Figure 3: Uranus flux density measurements obtained during the 4th GISMO pool. The horizontal black dashed line and the gray shaded area correspond to the median value and to the rms, respectively.

3 Sensitivity

During the three first days of the second week the opacity at 225 GHz was systematically $\lesssim 0.15$ (see Figure 4) thus allowing to study the behavior of GISMO under excellent conditions of atmospheric transparency barely experienced in previous pools (see appendix A). The NEFD measured for the scans collected during this period is higher than the NEFD measured for bad weather conditions.

This unexpected behavior[2] is clearly visible by comparing Figures 4 and 5. The anti-correlation between $\tau_{225\,\mathrm{GHz}}$ and the NEFD is also appreciable in Figure 6 as an increasing value of the NEFD for values of $\tau_{225\,\mathrm{GHz}}$ lower than ~ 0.2. In order to study quantitatively this behavior, data were split into the scans collected under good and bad weather conditions. As Table 2 shows, the median value of the NEFD is 25% higher for the scans taken under good weather.

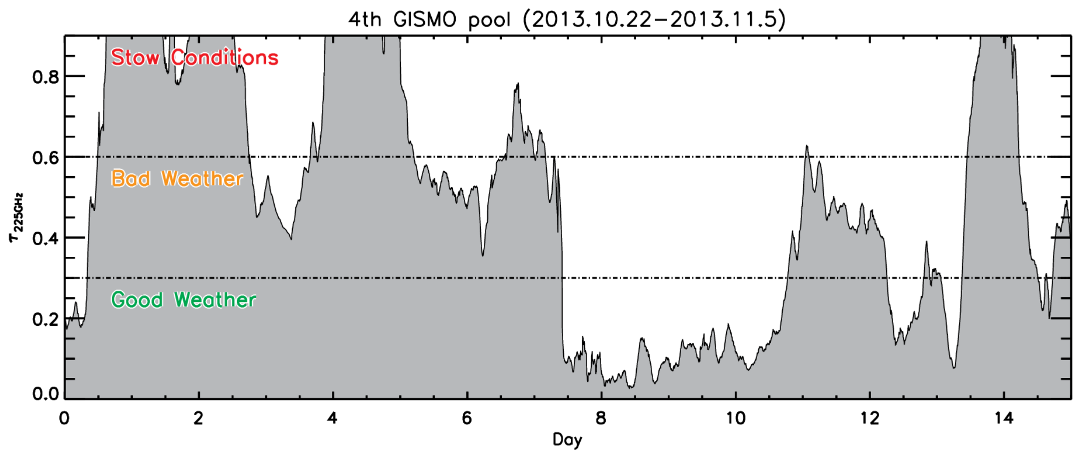

Figure 4: Taumeter readings during the 4th GISMO pool.

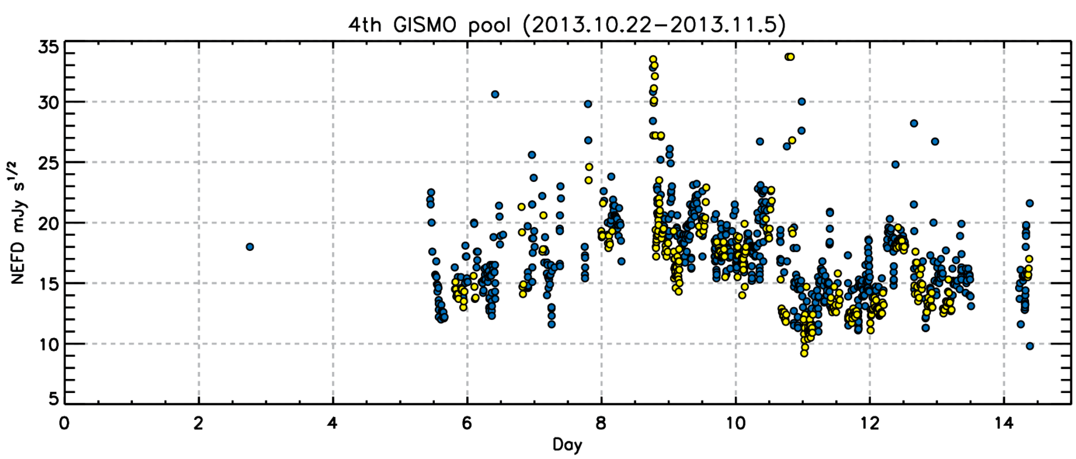

Figure 5: Values of the NEFD mesured during the 4th GISMO *vs* date. Blue filled circles correspond to scanning speeds under $60\,''/s$ and yellow to scanning speeds above $60\,''/s$.

It is important to note that the preceding analysis is based on the Nexus logsheet and therefore, data reduction was performed with crush v 2.15-1 and the `default` filtering option. In order to reject possible problems related with the version of crush or the filtering option, data from project 077-13 were reduced manually with crush v 2.15-2 and using both the `default` and the `faint` filtering options. As Figure 7 shows, in this case the NEFD is 50% higher for the scans taken under good weather conditions. This surprising behavior is currently being investigated by the GISMO team.

[2]The value of the NEFD calculated by crush does not include the atmospheric contribution, and therefore, variations with the opacity are not expected.

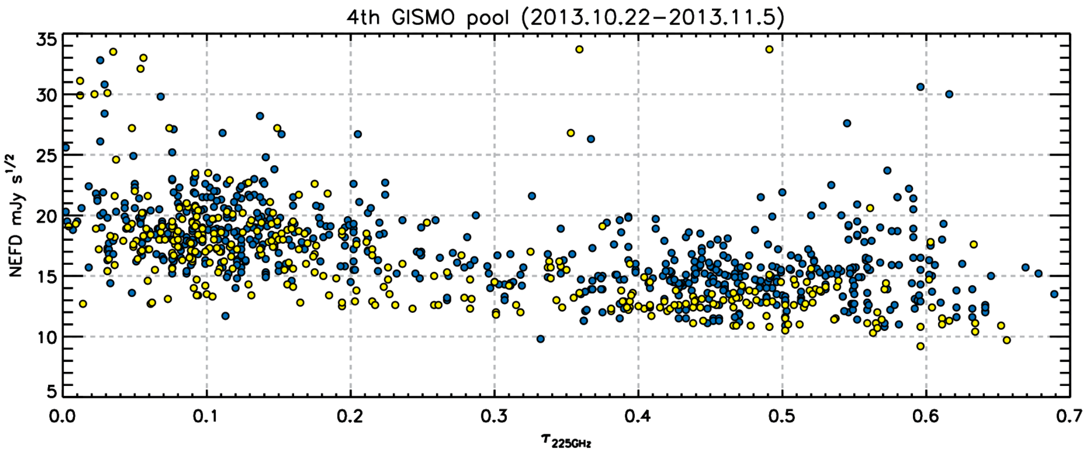

Figure 6: Values of the NEFD mesured during the 4th GISMO *vs* $\tau_{225\,GHz}$. Blue filled circles correspond to scanning speeds under $60''/s$ and yellow to scanning speeds above $60''/s$.

Queue	Number of scans	$\tau_{225\mathrm{GHz}}$	NEFD (mJy $\sqrt{\mathrm{s}}$)	Healthy channels
Bad weather	612	0.499	14.8	99
Good weather	601	0.105	18.5	102
Total	1213	0.307	16.8	101

Table 2: Total number of scans collected (column 2), median value of $\tau_{225\,\mathrm{GHz}}$ (column 3), median value of NEFD (column 4), and median value of healthy channels (column 5) for the good and the bad weather queus.

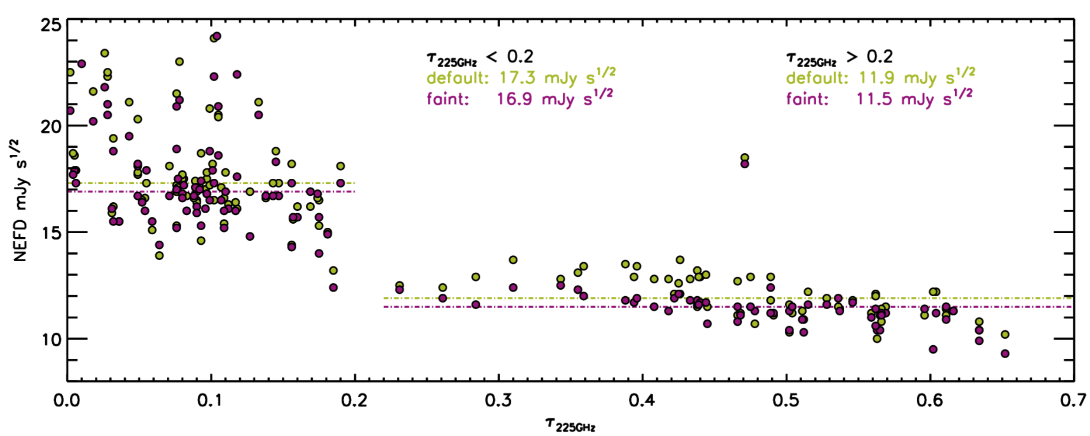

Figure 7: Values of the NEFD for the `default` and the `faint` filtering options based on data from project 077-13. Data were reduced with crush v 2.15-2.

4 Scientific analysis: NGC 1569

NGC 1569 is a low metallicity, dwarf starbursting galaxy located at a distance of 3.32 Mpc. The emission from NGC 1569 is completely dominated by its central star forming complex. This galaxy has been observed during the 4th GISMO pool (project 078-13) for a total of 58 minutes. The observations consisted on $4' \times 4'$ Lissajous maps. The scans were combined using crush v 2.15-2 and the filtering scheme `faint` (see Figure 8). The observed flux density was found to be 43.7 ± 2.6 mJy. In order to check the accuracy of this value, we compared the observed spectral energy distribution (SED) to the radiation transfer model of Groves et al. (2008). The best fit obtained is shown in Figure 9. The model fits the GISMO 2 mm data point nicely.

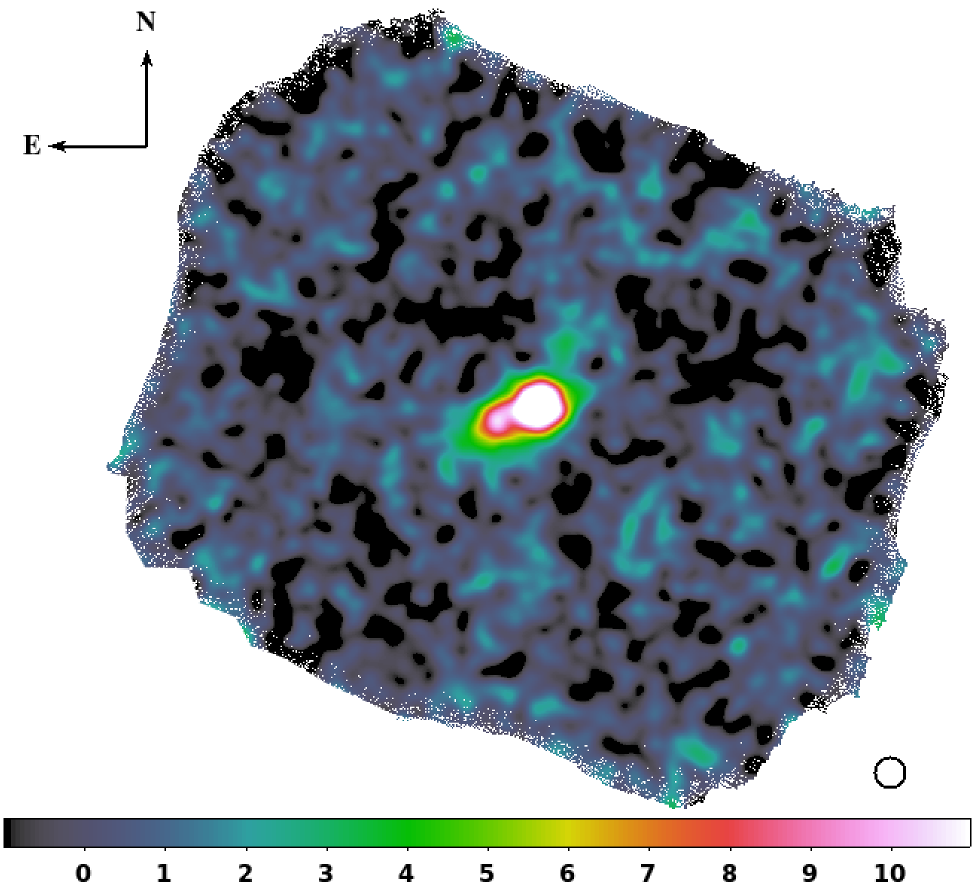

Figure 8: Signal to noise map of NGC 1569. The small circle at the right bottom corner corresponds to the final resolution of the image (21″).

References

Bendo, G. J., Griffin, M. J., Bock, J. J., et al. 2013, MNRAS, 433, 3062

Bruni, G., Kramer, C., Billot, N., & Quintana-Lacaci, G. 2012, IRAM 30 m documentation

Groves, B., Dopita, M. A., Sutherland, R. S., et al. 2008, ApJS, 176, 438

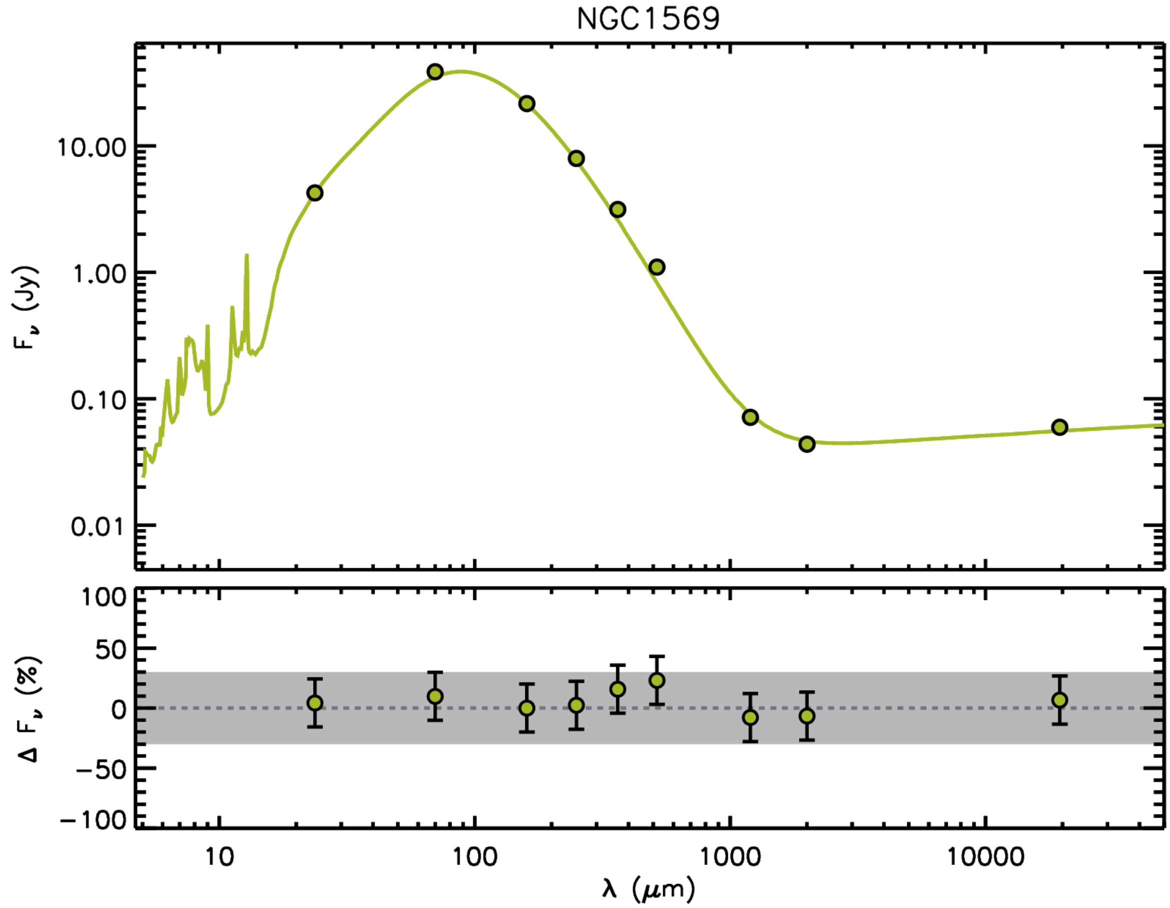

Figure 9: Spectral energy distribution of NGC 1569. From shorter to longer wavelengths, data points correspond to MIPS 24 μm, PACS 70 μm, PACS 100 μm, SPIRE 250 μm, SPIRE 350 μm, SPIRE 500 μm, MAMBO 1 mm, GISMO 2 mm, and RYLE 2 cm. Note that non-thermal emission was subtracted from RYLE 2 cm data following Kepley et al. (2010).

Hermelo, I., Kramer, C., Billot, N., & González, M. 2013, IRAM 30 m documentation

Kepley, A. A., Mühle, S., Everett, J., et al. 2010, ApJ, 712, 536

Sayers, J., Czakon, N. G., & Golwala, S. R. 2012, ApJ, 744, 169

A NEFD from previous pools

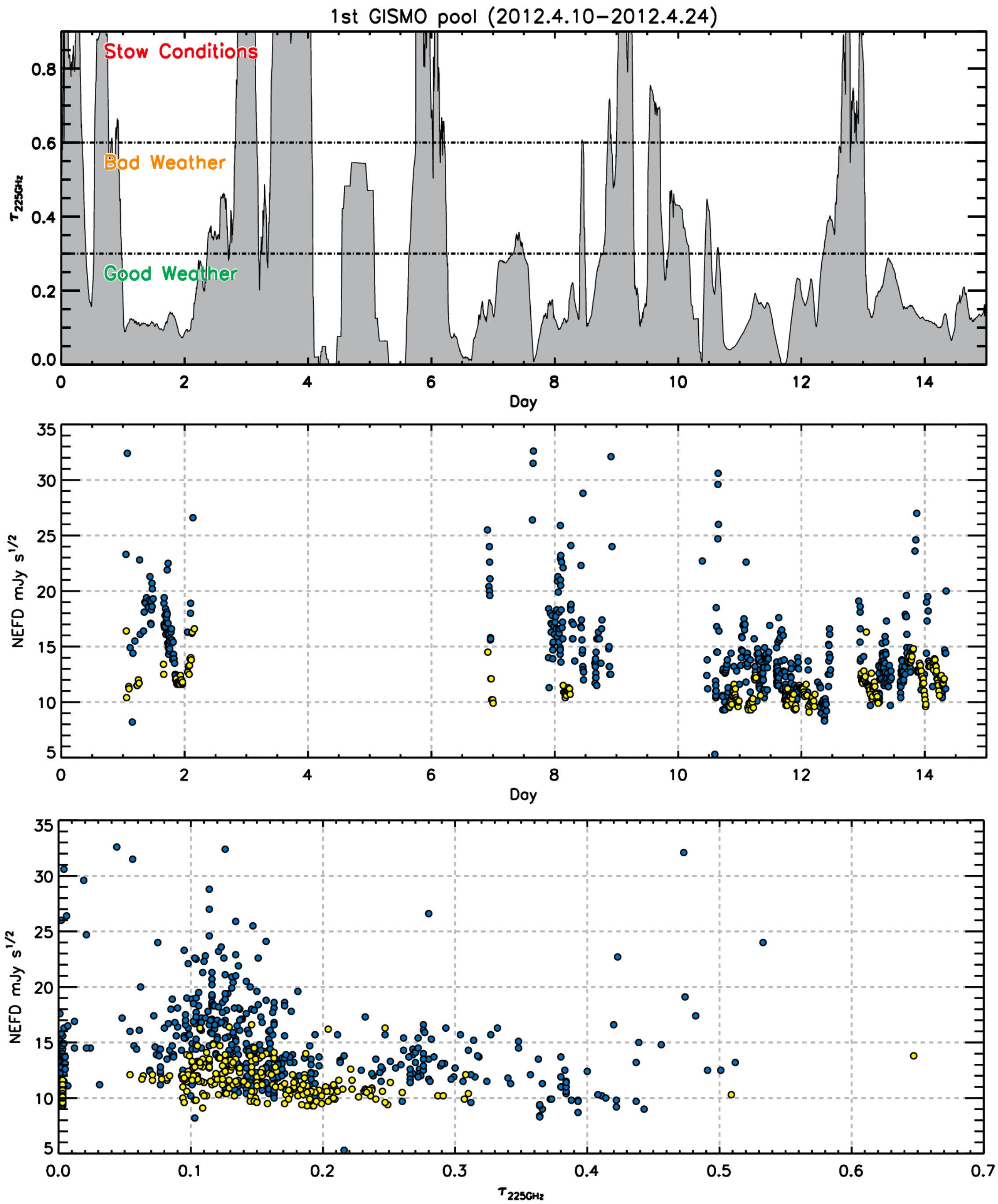

Figure A.1: Same as Figures 4, 5 and 6 for the 1st GISMO pool.

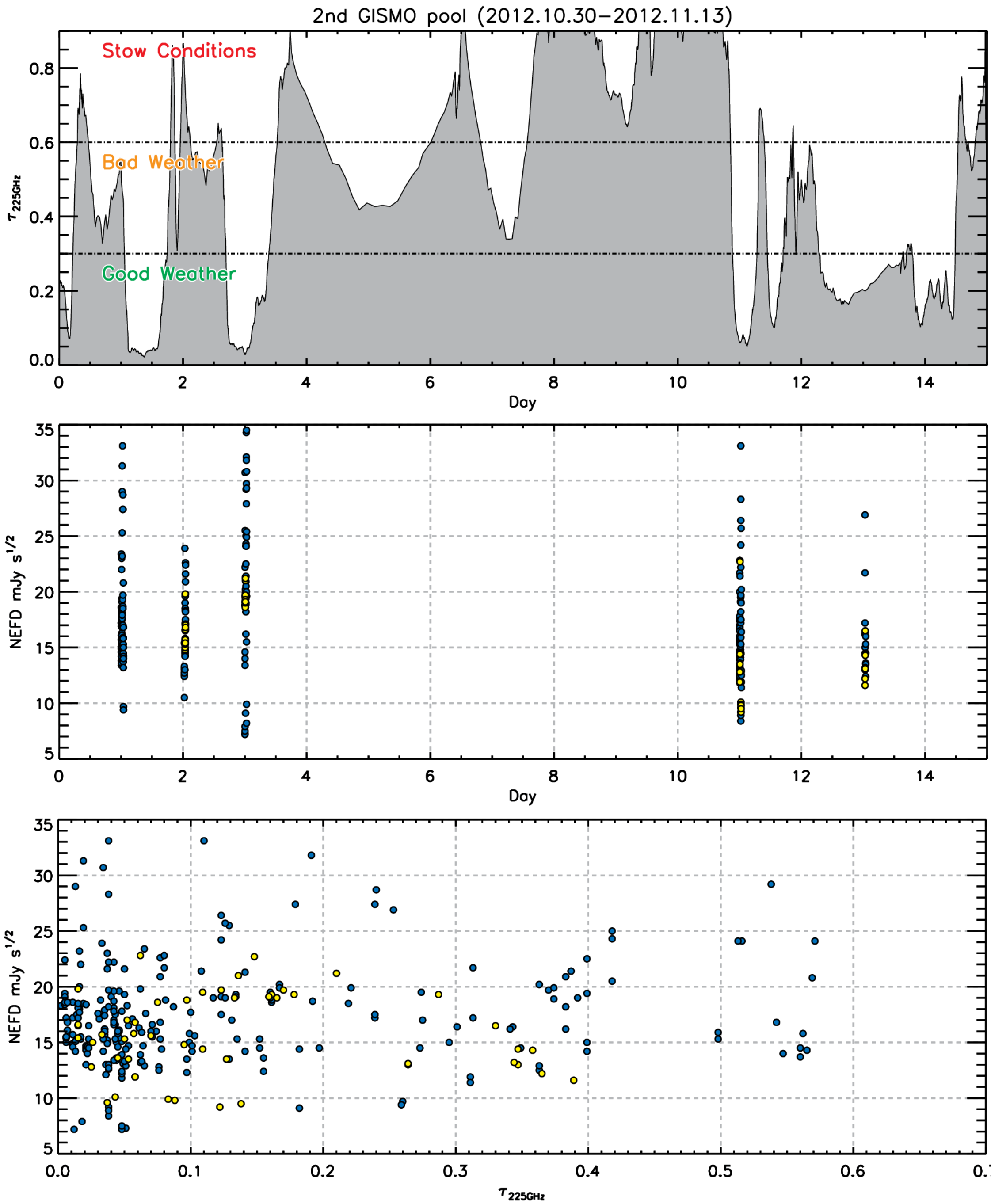

Figure A.2: Same as Figures 4, 5 and 6 for the 2nd GISMO pool.

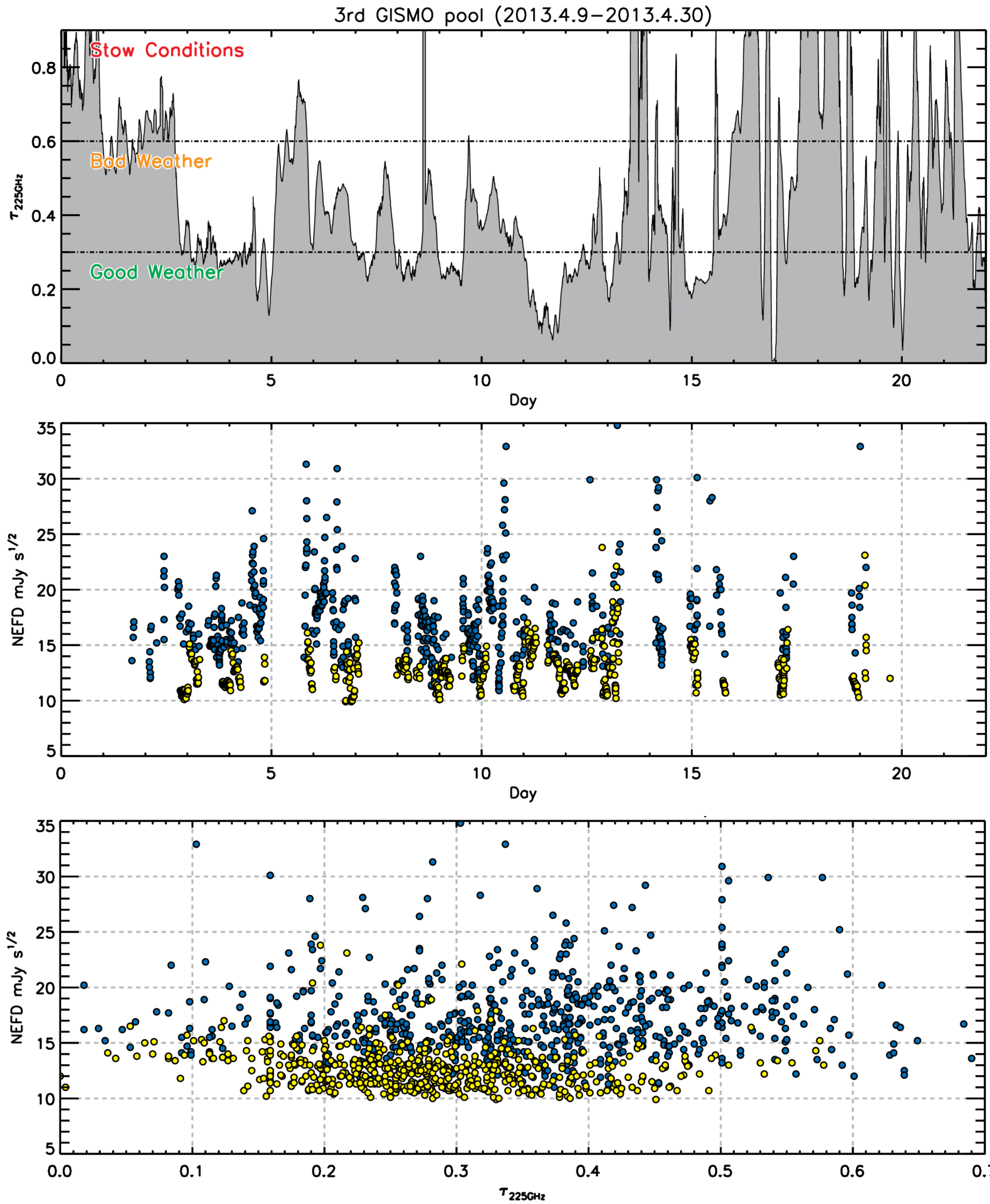

Figure A.3: Same as Figures 4, 5 and 6 for the 3rd GISMO pool.